Theoretical Studies of Blue-Emitting Iridium Complexes with Different Ancillary Ligands

Xin Gu,[†] Teng Fei,[†] Houyu Zhang,*[,†] Hai Xu,[†] Bing Yang,[†] Yuguang Ma,*[,†] and Xiaodong Liu[‡]

State Key Laboratory of Supramolecular Structure and Materials, Jilin University, Changchun 130012, People's Republic of China, and College of Chemistry, Jilin University, Changchun 130012, People's Republic of China

Received: March 27, 2008; Revised Manuscript Received: June 23, 2008

The structural and electronic properties of two heteroleptic iridium complexes $Ir(dfppy)_2(pic)$ (FIrpic) and $Ir(dfppy)_2(acac)$ (FIracac) have been investigated theoretically, where dfppy = 2-(2,4-difluorophenyl) pyridine, pic = picolinic acid, and acac = acetoylacetonate. The geometries of ground and excited states are optimized at PBE0/LANL2DZ and CIS/LANL2DZ levels, respectively. Time-dependent density functional theory (TDDFT) method is employed to explore the absorption and emission properties. In the ground state, the highest-occupied molecular orbital has a significant mixture of metal Ir(d) and dfppy(π), the lowest-unoccupied orbital locates primarily on π^* of pic for FIrpic and π^* of dfppy for FIracac. The luminescence of each complex originates from the lowest triplet excited state, which is assigned to the mixing of metal-to-ligand charge transfer and intraligand charge transfer characters. The effects of ancillary ligands pic and acac on absorption and emission spectra are observed by analysis of TDDFT results. The connection between the nature of excited states and the behavior of the complexes with different ancillary ligands is elucidated.

Introduction

Luminescent d^6 transition metal complexes of Re(I),[1] Ru(II),[2] Os(II),[3] and Ir(III)[4]have attracted considerable attention due to their intriguing photophysical, photochemical, and excited-state redox properties and potential practical applications such as in solar energy conversion,[5] organic light-emitting diodes (OLEDs),[6] and sensors.[7] Among these complexes, iridium complexes are regarded as the most effective materials in OLEDs because of their high thermal stability, short lifetime in excited states, and strong spin−orbital coupling effect of heavy metal.[8] Moreover, the emission color can be tuned from red to blue through ligation of different ancillary ligands[9]or introducing a variety of donating or accepting groups on the ligands.[10] However, achieving room-temperature blue phosphorescence with high quantum efficiency remains as a challenge.[11] To attain blue emission, it is indispensable to select suitable chelate ligands with sufficiently large ligand-centered (LC) $\pi-\pi^*$ transition energies and/or metal-to-ligand charge transfer (MLCT) energies. Strong field ligands such as cyanide, carbonyl, and phosphine groups are introduced in the coordination sphere to increase the energy gap between the highest-occupied molecular orbital (HOMO) and lowest-unoccupied molecular orbital (LUMO) and to achieve hypsochromic shift in the emission.[8a,10a,12] But it might inevitably increase the chance of nonradiative decay since LC $\pi-\pi^*$ transition (or MLCT) reaches the region closed to higher-lying metal-centered (MC) dd states, which might affect the efficiency of blue Ir(III) complexes, resulting in weak-emissive or nonemissive at room temperature. To achieve Ir(III) complexes in which light emission predominates over nonradiative decay, choosing congruent ancillary ligands is a feasible approach to suppress the activation of MC dd states and enhance the blue phosphorescence.[13]

* To whom correspondence should be addressed. E-mail: houyuzhang@jlu.edu.cn (H.Z.); ygma@jlu.edu.cn (Y.M.).

† State Key Laboratory of Supramolecular Structure and Materials, Jilin University.

‡ College of Chemistry, Jilin University.

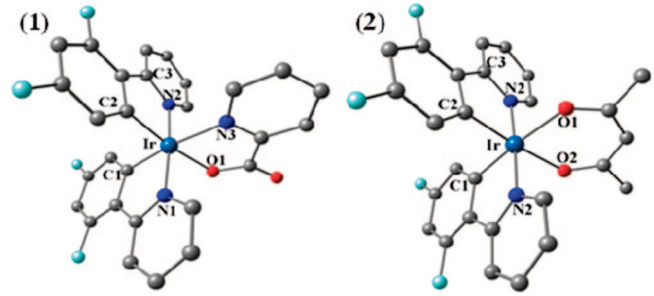

Figure 1. Optimized geometry structures of FIrpic (1) and FIracac (2) with two N atoms in dfppy at the trans position. (Saturated H atoms are not shown.)

Recently, the iridium complexes with formula $[Ir(C^N)_2(L^X)]$ (C^N = dfppy, 2-phenylpyridinato; L^X = ancillary ligands) were designed and synthesized in a systematic manner to explore the effects of ancillary ligands on the excited-state properties.[10b] Spectroscopic data analysis for $Ir(C^N)_2(L^X)$ revealed that different ancillary ligands L^X alter the ^{1}MLCT energy mainly by changing the HOMO energy level. In contrast to the experimental studies, so far theoretical efforts on deep understanding phosphorescent emission seem deficient, especially on the excited-state behavior of the metal complexes. Though density functional theory (DFT) calculations have been performed on large numbers of luminescent metal complexes to evaluate a variety of ground-state properties with an accuracy close to that of experimental electrochemical measurements,[14] only a few excited-state calculations using TDDFT on Ir(III) complexes have been reported.[15] Because of high computational cost, it is usually hard to obtain the excited-state geometry. The emission properties have to be calculated based on the ground-state geometry, which is assumed that the geometry does not change much between the ground and excited states. Our motivation is to get geometries of excited-state and spectroscopic properties related to the excited state.

As far as DFT approaches are concerned, the "hybrid" density functionals[16]such as B3LYP, B3PW91, and PBE0 combining

10.1021/jp8026429 CCC: $40.75 © 2008 American Chemical Society
Published on Web 08/15/2008

TABLE 1: Main Optimized Parameters of Complexes in the Ground State S_0 and the Lowest-Lying Triplet Excited State T_1 at PBE0 and CIS Levels, Respectively, Together with Experimental Values of FIrpic

	FIrpic				FIracac	
	S_0[a]	S_0[b]	exptl[c]	T_1[b]	S_0[b]	T_1[b]
Bond Lengths (Å)						
Ir−C1	1.997	2.005 (2.013)[d]	1.996	2.039	1.988	2.032
Ir−N1	2.047	2.041 (2.072)	2.043	2.096	2.031	2.084
Ir−C2	1.991	1.995 (2.011)	1.991	2.043	1.998	2.033
Ir−N2	2.037	2.030 (2.062)	2.023	2.074	2.031	2.079
Ir−O1	2.156	2.144 (2.180)	2.174	2.146		
Ir−N3	2.168	2.134 (2.211)	2.126	2.199		
Ir−O1					2.147	2.162
Ir−O2					2.147	2.163
Bond Angles (Deg)						
N1−Ir−N2	175.4	175.4	175.5	175.2	177.4	176.7
C1−Ir−C2	90.4	90.4	88.0	90.1	92.9	91.9
O1−Ir−N3	77.0	77.6	77.1	75.8		
O1−Ir−O2					86.8	83.3
Dihedral Angles (Deg)						
C3−N2−Ir−N3	−92.7	−94.9	−99.6	−96.4		
C3−N2−Ir−O1					−85.3	−89.4

[a] PBE0/genECP calculation results. [b] PBE0/LANL2DZ calculation results. [c] From ref 28. [d] Values in parentheses are from ref 27.

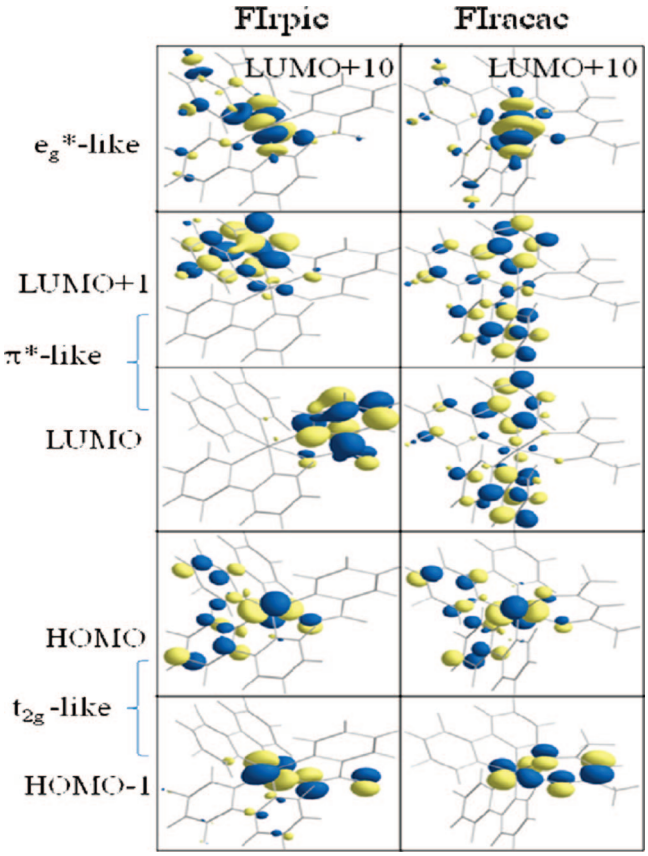

Figure 2. Contour plots of frontier orbitals and e_g*-like d orbitals of FIrpic and FIracac in ground states.

"exact exchange" with gradient-corrected density functional are often used. PBE0[17]is a hybrid HF/DFT approach based on the Perdew−Burke−Erzenrh (PBE)[18]functional, which is considered a reliable DFT method to describe both covalent interactions and systems containing heavy atoms.[17] TDDFT with PBE0 functional is able to give accurate excitation energies.[19] The configuration interaction singlets (CIS)[15e,20] method is commonly used in optimizing the excited states. Rich excited-state information would provide quantum chemical insights on the understanding the optical and photophysical properties of metal complexes and inspire a new thought on designing novel metal complexes.[21]

The optical properties of the cyclometalated Ir(III) complexes are strongly dependent on the characteristics of their ground and lowest-lying excited states. In this work, we perform quantum calculations on two blue-emitting iridium complexes toward better understanding of the phosphorescent behavior and thus acquiring the knowledge on how to improve luminescence efficiency. By analysis of orbital compositions and transition characters of the complexes, we can explore the nature of absorption and emission properties. We strongly desire to understand the interaction between metal and ligands and how to alter the optical properties by appropriate ligands. As the effect of ligation on luminescent behavior becomes better understood, it will become possible to predict the properties of light emission for a novel complex from its structural design.

Computational Details

Ground-state geometries for the two complexes are fully optimized without any symmetry constrains by DFT calculations using the PBE0 model. Two kinds of basis sets ("double-ζ" quality basis sets with 6-31g(d)[22]for ligands and LANL2DZ for Ir (referred to as genECP); LANL2DZ for all elements) are employed for comparison on the geometry optimization, and PBE0/LANL2DZ is finally chosen for all calculations in this paper. A relativistic effective core potential (ECP)[23]on Ir replaced the inner core electrons leaving the outer core $[(5s)^2(5p)^6]$ electrons and the $(5d^6)$ valence electrons of Ir(III). CIS approach is employed to optimize the geometry structures in the triplet excited states (T_1). To obtain the vertical excitation energies of the low-lying singlet and triplet excited states of the complexes, TDDFT calculations using the PBE0 functional are performed at the optimized ground-state (S_0) geometry and excited-state (T_1) geometry, respectively. Ten singlet excited states and 10 triplet excited states are calculated. The calculated results are compared with the experimental absorption and emission data. Ligands of dfppy, acac, and pic are optimized at the PBE0/6-31g(d) level to obtain the frontier-orbital energy levels. According to previous study,[24] only the most stable structures in which two N atoms in dfppy ligands at trans position are considered. All calculations are carried out using the Gaussian 03 package.[25]

TABLE 2: Molecular Orbital Compositions in the Ground States for FIrpic and FIracac at the PBE0/LANL2DZ Level

			MO composition (%)				
	orbital	energy (eV)	Ir	dfppy(1)	dfppy(2)	pic/acac	main bond type
FIrpic	LUMO+2	−1.90	3.82	9.11	83.7	3.37	π*(dfppy)
	LUMO+1	−2.03	4.41	83.5	8.13	3.93	π*(dfppy)
	LUMO	−2.20	1.67	3.16	2.50	92.7	π*(pic)
	HOMO	−6.12	45.3	21.2	24.8	8.72	d(Ir) + π(dfppy)
	HOMO-1	−6.54	50.6	11.8	14.9	22.6	d(Ir) + π(dfppy) + π(pic)
	HOMO-2	−6.92	26.7	32.7	34.7	5.90	d(Ir) + π(dfppy)
FIracac	LUMO+2	−1.37	3.94	7.22	7.23	81.6	π*(acac)
	LUMO+1	−1.76	3.64	45.3	49.6	1.45	π*(dfppy)
	LUMO	−1.78	3.60	48.9	44.6	2.95	π*(dfppy)
	HOMO	−5.82	48.1	22.0	22.0	7.79	d(Ir) + π(dfppy)
	HOMO-1	−6.19	43.9	7.78	7.79	40.5	d(Ir) + π(acac)
	HOMO-2	−6.66	57.4	18.1	18.2	6.24	d(Ir) + π(dfppy)
	HOMO-3	−6.75	0.36	47.1	47.4	5.14	π(dfppy)

Results and Discussion

Molecular Structures in Ground-State S_0 and Triplet Excited-State T_1. The complexes FIrpic and FIracac have the same dfppy ligands in the coordination with distorted octahedral configuration. Because of different ancillary ligands, they possess C1 and C2 symmetry, respectively. The optimized ground-state geometry structures of FIrpic and FIracac are shown in Figure 1, and the optimized geometrical parameters in both ground-state S_0 and triplet excited-state T_1 are reported in Table 1, together with available experimental X-ray diffraction data of FIrpic. The calculated ground-state geometrical parameters of FIrpic by using different basis set are summarized for comparison with the experimental data. The results from basis sets LANL2DZ for all atoms and mixed basis sets genECP are in good agreement with available crystal structural data. The calculated standard deviations[26] for the bond lengths are 0.020 Å for LANL2DZ and 0.015 Å for genECP, and the standard deviations for the bond angle are 0.72° for LANL2DZ and 0.67° for genECP. The calculated parameters are consistent with previous results.[27] Thus it is reasonable to use LANL2DZ basis set for rest of calculation for saving computational cost, especially for optimization of the excited states.

Structurally, all three chelate ligands show bite angles of 76.3−80.4° for FIrpic and 80.6−86.4° for FIracac. In complex FIrpic, it is notable that the dfppy ligands adopt mutually an eclipsed configuration with the nitrogen atoms N1 and N2 residing at the trans location and bond lengths of Ir−N are 2.041 and 2.030 Å, respectively. Atoms C1 and C2 are in the cis position on the Ir atom with the Ir−C distance 2.005 and 1.995 Å. The angles of N1−Ir−N2 and C1−Ir−C2 are 175.4 and 90.4°, respectively. Complex FIracac compound has the same configuration of dfppy ligands with almost equivalent Ir−N (C) bond lengths due to the C2 symmetry. We are interested in the interaction of centric Ir metal with the ancillary ligands pic and acac. The bond length of Ir−O1 (2.144 Å) in FIrpic is almost the same as that of Ir−O2 (2.147) in FIracac, while the bond length Ir−N3 (2.134 Å) in FIrpic is shorter than the counterpart of Ir−O1 (2.147 Å) in FIracac. We can conclude that pic is a stronger ligand that can bind tightly with the centric Ir atom through Ir−N bond in comparison with acac. This is also reflected from Ir−C1 bond lengths changes in the complexes. FIrpic displays a slightly elongated Ir−C1 distance of 2.005 Å (1.998 Å in FIracac). This is believed to be caused by the stronger Ir−N3 bonding interaction of the pic ligand, which eventually weakened the Ir−C1 bond at its trans disposition.

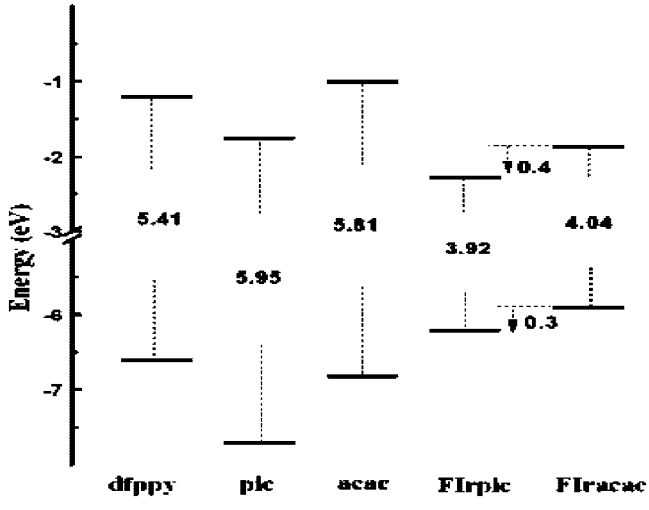

Figure 3. Energy gaps of ligands and iridium complexes.

Upon excitation, the complexes experience vertical transition from ground state to singlet excited state and then undergo intersystem crossing to reach the triplet excited state in which phosphorescence might occur. According to structure−property relationship, the structural changes would be expected between the S_0 and T_1 states. The comparison of the S_0 and T_1 states geometries shows that, in the T_1 excited state, the metal−ligand bond lengths have perceptible changes. For example, the calculated Ir−N and Ir−C bonds have about 0.05 Å elongation, while Ir−O bonds have about 0.02 Å elongation. The calculated bond angles and dihedral angles show only a slight change of about 1−3°.

Molecular Orbitals in Ground States. The features of the frontier orbitals of FIrpic and FIracac in ground states are depicted in Figure 2, and the descriptions of molecular orbital composition and main bond type are summarized in Table 2. Apparently, the electron densities of the ground state of FIrpic complex for HOMO, HOMO-1, and HOMO-2 are mainly based on dfppy moieties and the Ir atom, in which the contribution from metal 5d orbitals are 45.3, 50.6, and 26.7%, respectively. According to ligand field theory, HOMOs comprising apparent 5d character can be considered as "t_{2g}" orbitals. It is easy to recognize from the contour plot of Figure 2 that HOMOs are mainly composed by d_{xy}, d_{yz}, and d_{zx}. The associated e_g*-like orbital is over 6.93 eV higher in energy, which is recognized as LUMO+10 with energy 0.81 eV. It is notable that such a large d-orbital splitting is attainable for third row transition metal ions, which makes ligand-based color tuning in these complexes possible. Below the vacant metal centered e_g*-like orbitals, there exist some ligand centered π* orbitals that determine the emissive transition. In complex FIrpic, the LUMO is almost

TABLE 3: Calculated Excited Energies, Dominant Orbital Excitations, and Oscillator Strength (*f*) from TDDFT Calculations for the FIrpic Complex

state	excitation	E_{cal} (eV)	λ_{cal} (nm)	*f*	λ_{exp}[a] (nm)	character
Singlet Excited States						
S_1	HOMO→LUMO (0.68)	2.99	415	0.0023		Ir/dfppy→pic(MLCT/LLCT)
S_2	HOMO→LUMO+1 (0.66)	3.11	398	0.0294	390	Ir/dfppy→dfppy(MLCT/ILCT)
S_3	HOMO→LUMO+2 (0.67)	3.25	382	0.0076		Ir/dfppy→dfppy(MLCT/ILCT)
S_4	HOMO-1→LUMO (0.66)	3.37	368	0.0151		Ir/pic/dfppy→pic(MLCT/ILCT/LLCT)
S_8	HOMO-1→LUMO+2 (0.61)	3.72	333	0.0916		Ir/pic/dfppy→dfppy(MLCT/LLCT/ILCT)
S_9	HOMO-2→LUMO (0.45)	3.83	324	0.0736		Ir/dfppy →pic(MLCT/LLCT)
	HOMO-3→LUMO (0.40)					Ir/dfppy/pic→pic(MLCT /LLCT/ILCT)
Triplet Excited States						
T_1	HOMO→LUMO+1 (0.49)	2.75	451			Ir/dfppy→dfppy(MLCT/ILCT)
T_2	HOMO→LUMO+2 (0.41)	2.79	445			Ir/dfppy→dfppy(MLCT/ILCT)
	HOMO-1→LUMO+2 (0.31)					Ir/pic/dfppy→dfppy(MLCT/ILCT)
T_3	HOMO-1→LUMO (0.52)	2.90	427			Ir/pic→pic(MLCT/ILCT)
	HOMO→LUMO (0.34)					Ir/dfppy→pic(MLCT/LLCT)

[a] Form ref.[28]

TABLE 4: Calculated Excited Energies, Dominant Orbital Excitations, and Oscillator Strength (*f*) from TDDFT Calculations for the FIracac Complex

state	excitation	E_{cal} (eV)	λ_{cal} (nm)	*f*	λ_{exp}[a] (nm)	character
Singlet Excited States						
S_1	HOMO→LUMO+1 (0.68)	3.06	406	0.0346	387	Ir/dfppy→dfppy(MLCT/ILCT)
S_3	HOMO-1→LUMO (0.68)	3.41	363	0.0473		Ir/acac→ dfppy(MLCT/LLCT)
S_6	HOMO→LUMO+3 (0.68)	3.74	331	0.0137		Ir/dfppy→ acac(MLCT/LLCT)
S_7	HOMO-1→LUMO+2 (0.50)	3.81	325	0.0635		Ir/dfppy→ fppy(MLCT/ILCT)
	HOMO-2→LUMO+1 (0.39)					Ir/dfppy→dfppy(MLCT/ILCT)
S_9	HOMO-2→LUMO+1 (0.51)	3.89	318	0.0438		Ir/dfppy→dfppy(MLCT/ILCT)
S_{10}	HOMO-2→LUMO (0.46)	3.91	317	0.0097		Ir/dfppy→dfppy(MLCT/ILCT)
Triplet Excited States						
T_1	HOMO→LUMO+1 (0.56)	2.71	457			Ir/dfppy→dfppy(MLCT/ILCT)
	HOMO-3→LUMO (0.29)					dfppy →dfppy(ILCT)
T_2	HOMO→LUMO (0.55)	2.72	455			Ir/dfppy→dfppy(MLCT/ILCT)
	HOMO-3→LUMO+1 (0.31)					dfppy →dfppy(ILCT)
T_3	HOMO-1→LUMO+2 (0.70)	2.81	442			Ir/acac→ acac(MLCT/ILCT)

[a] From ref 10c.

exclusively located on the π-system of the pic ligand, as can be seen in Figure 2. The electron densities in LUMO+1 and LUMO+2 are localized in dfppy ligands. These LUMOs are ligand−π* orbitals. No significant interaction between the ligand and the metal-centered orbitals can be observed in the LUMOs. For complex FIracac, HOMOs mainly come from Ir 5d orbitals, with significant admixture of ligand dfppy π character, similar with that in FIrpic. The LUMO electron densities are mainly contributed from ligand dfppy π* orbitals. The e_g*-like orbital is 6.81 eV above the HOMO. In a previous study, the emission color tuning was usually based on the adjustment of the HOMO−LUMO energy gaps.[9,10] LUMO energy can be adjusted through deliberate chemical synthesis to allow for emission colors across the visible spectrum. But the e_g*-like orbital above the LUMOs will affect the luminescent efficiency.

From Figure 3 we can see that ancillary ligands pic and acac are satisfied with large ligand-centered $\pi-\pi$* transition energies 5.95 and 5.81 eV compared with 5.41 eV for dfppy. The interaction of centric Ir atom with two kinds of ligands could be very complicated. Ligand pic has very low HOMO and LUMO energy levels, and a wide HOMO−LUMO energy gap could afford strong ligand field to metal Ir. Because of the strong interaction between the pic and Ir atom, the ligand pic dominates the energy level of LUMO and is partly involved in HOMO and HOMO-1. Such interaction could lower the LUMOs apart from the e_g* orbitals and decease the energy levels of HOMOs to get large transition energy. While ligand acac takes part in the formation of LUMO+2 and HOMO-1 of FIracac, it has less effect on the HOMO and LUMO. We can conclude that ancillary ligand pic has great effect on both the HOMO and LUMO. The energy levels of the HOMO and LUMO of FIrpic decrease by 0.3 and 0.4 eV in comparison with those of FIracac, respectively. This can be ascribed to lower HOMO and LUMO energy levels of the pic ligand and a strong interaction between the pic and Ir atom.

Absorption Properties. The results from TDDFT calculations for FIrpic and FIracac at optimized ground-state geometries are shown in Tables 3 and 4. For each complex, we give the vertical excitation energies for the lowest 10 singlet and 3 triplet states, together with the characters of the transition. From Table 3 for the complex FIrpic, we can see that the excitation energy for the lowest triplet state T_1 is 2.75 eV. This corresponds to excitation from the HOMO with significant dπ character (Ir(d) 45% + dfppy(π) 46%) to LUMO+1 with almost π* orbital of dfppy ligands (84%). The corresponding singlet state is found about 0.36 eV higher in energy for S_2. According to the assignments, we would label the lowest excited state as a mixed state of MLCT state and intraligand charge transfer (ILCT) state. Triplet excited-state T_2 is also charactered as mixed MLCT and ILCT states. Thus the charge transition involved in the absorption process can be described as [d(Ir)+ π(dfppy) → π*(dfppy)]. It is worth noting that, at higher excited states such as S_4, there exists admixture of MLCT and ligand−ligand charge transfer (LLCT) states.

For the complex FIracac, two triplet excited states T_1 and T_2 with extremely close energy (within 0.01 eV) are involving two

TABLE 5: Molecular Orbital Compositions in the Excited States for FIrpic and FIracac at the CIS/LANL2DZ Level

			MO composition (%)				
	orbital	energy (eV)	Ir	dfppy(1)	dfppy(2)	pic/acac	main bond type
FIrpic	LUMO+2	−1.81	3.32	6.32	88.1	2.24	π*(dfppy)
	LUMO+1	−2.01	2.21	2.55	2.95	92.3	π*(pic)
	LUMO	−2.20	2.83	89.6	4.47	3.07	π*(dfppy)
	HOMO	−6.09	46.8	21.3	21.5	10.4	d(Ir) + π(dfppy)
	HOMO-1	−6.52	52.8	11.0	10.1	26.1	d(Ir) + π(dfppy) + π(pic)
	HOMO-2	−6.78	23.6	59.8	13.1	3.57	π(dfppy) + d(Ir)
FIracac	LUMO+2	−1.14	1.17	14.5	83.8	0.51	π*(dfppy)
	LUMO+1	−1.69	3.31	5.76	89.6	1.37	π*(dfppy)
	LUMO	−1.93	2.95	91.3	4.52	1.22	π*(dfppy)
	HOMO	−5.81	49.6	21.7	18.8	9.86	d(Ir) + π(dfppy) + π(acac)
	HOMO-1	−6.07	38.3	6.10	5.56	50.0	π(acac) + d(Ir) + π(dfppy)
	HOMO-2	−6.55	25.6	59.8	8.70	5.90	π(dfppy) + d(Ir)

types of transitions. Transitions from HOMO to LUMO and LUMO+1 belong to the mixture of MLCT and ILCT states [d(Ir)+π(dfppy) → π*(dfppy)], while transitions from HOMO-3 to LUMO and LUMO+1 are almost complete ILCT [π(dfppy) → π*(dfppy)] transition character. For the T_3 state, it has [d(Ir) + π(acac) → π*(acac)] transition character.

Triplet Excited-State and Emission Properties. Besides the structural changes between the ground and excited states, the electronic properties in the triplet excited-state also varied with structural relaxation, as shown by the results at the optimized T_1 state geometries for the respective molecules in Tables 4 and 5. The frontier molecular orbital composition and main bond type from the ground S_0 state at the T_1 geometry are listed in Table 5, and pictorial orbitals are shown in Figure 4. Both complexes have similar HOMOs to those at the ground-state geometry. For the complex FIrpic, LUMO mainly localizes in dfppy, and LUMO+1 localizes in pic, which is contrary to that in the ground state. This change in the character of the LUMO and LUMO+1 in comparing the S_0 and T_1 geometries agrees with the previous study.[27] LUMOs in FIracac keep the same features as that in the ground state. The MC centered "e_g*" orbital apparently goes downward, especially for complex FIracac. Such behavior is not good since MC-centered dd states will quench the emission in the triplet states resulting in radiationless transition.

The emission energies and dominant transitions from TDDFT calculations for complexes FIrpic and FIracac at optimized triplet excited-state geometries are presented in Table 6. The predicted emission wavelengths deviate from the experimental data by about 54 and 40 nm, respectively. For the two complexes, the lowest-lying excited states involve the dominant transition from LUMO to HOMO and LUMO to HOMO-2. From the orbital compositions listed in Table 5, we can see that LUMO and LUMO+2 predominantly locate at the π* orbital of ligand dfppy. HOMO and HOMO-2 have the mixed [d(Ir) + π(dfppy)] character. Thus we conclude that emission transition characters are from d(Ir)+ π(dfppy) to π*(dfppy).

Comments on Efficiency. From experimental results, we know that the efficiency of FIracac is not as excellent as that of FIrpic.[29] Combined with our calculated results, we conclude two possible reasons here. Because of the strong interaction between pic and the metal center, pic affects greatly on frontier orbitals in both the ground state and the excited state. Compared with the influence on HOMOs, ligand pic has a prominent effect on the LUMOs in FIrpic. In the triplet excited state, accompanied with largely structural relaxation, pic decreases the LUMO energy level dramatically by exchanging LUMO and LUMO+1 character, which is not found in FIracac. The more stable LUMO orbital with low energy in the excited state will definitely decrease the possibility of nonradiative decay through higher thermally activated MLCT states and MLCT to dd states conversion. Another possible reason is that the interligand charge transfer is not beneficial for high phosphorescence quantum efficiency.[30] As it can be seen from Figure 5, due to the symmetric ancillary ligands in FIracac, for the LUMO orbital, the electronic densities locate on two dfppy ligands upon excitation. But the electronic densities only locate on one dfppy ligand after the intersystem crossing process to emissive triplet states. We believe that the energy will dissipate during the

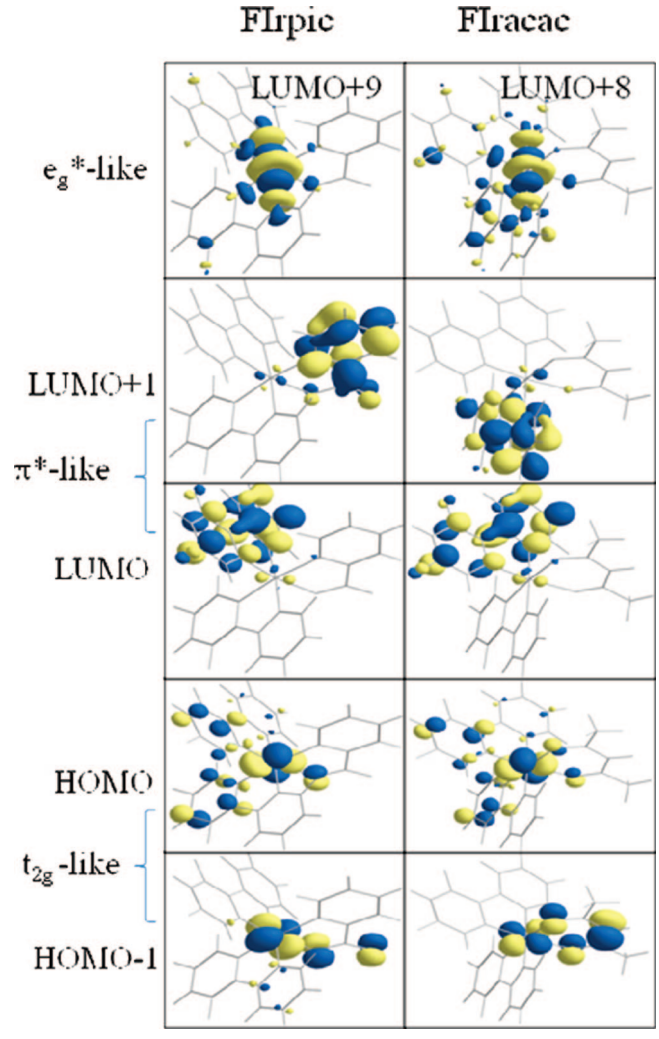

Figure 4. Contour plots of frontier orbitals and e_g*-like d orbitals of FIrpic and FIracac in excited states.

TABLE 6: Calculated Emission Energies and Dominant Orbital Emissions from TDDFT Calculations for Complexes FIrpic and FIracac

state	excitation	E_{cal} (eV)	λ_{cal} (nm)	λ_{exp} (nm)	character
FIrpic					
T_1	HOMO-2→LUMO (0.54)	2.37	522	468[a]	dfppy/Ir→dfppy(/LLCT /MLCT)
	HOMO→LUMO (−0.48)				Ir/dfppy/pic→dfppy(MLCT/ILCT)
T_2	HOMO→LUMO (0.37)	2.91	426		Ir/dfppy/pic→dfppy(MLCT/ILCT)
	HOMO→LUMO+2 (−0.32)				Ir/dfppy/pic→dfppy(MLCT/ILCT)
T_3	HOMO→LUMO+2 (0.34)	2.95	420		Ir/dfppy/pic→dfppy(MLCT/ILCT)
	HOMO→LUMO (0.34)				Ir/dfppy/pic→dfppy(MLCT/ILCT)
FIracac					
T_1	HOMO→LUMO(0.51)	2.38	522	482[b]	Ir/dfppy→dfppy(MLCT/ILCT)
	HOMO-2→LUMO (−0.51)				dfppy/Ir→dfppy(ILCT /MLCT)
T_2	HOMO→LUMO+1 (0.53)	2.85	435		Ir/dfppy→dfppy(MLCT/ILCT)
	HOMO-3→LUMO+1 (0.27)				Ir/dfppy→dfppy(MLCT/ILCT)
T_3	HOMO→LUMO (0.44)	2.89	429		Ir/dfppy→dfppy(MLCT/ILCT)
	HOMO-2→LUMO (0.34)				Ir/dfppy→dfppy(MLCT/ILCT)

[a] From ref[9] c. [b] From ref[10] c.

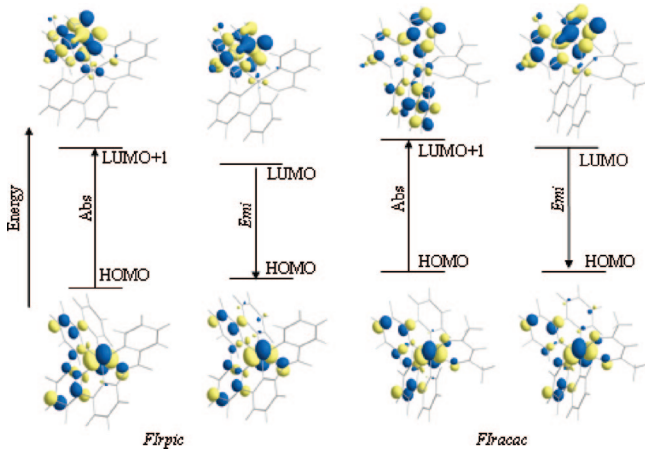

Figure 5. Transition contributions for the lowest-lying absorptions and emissions of the complexes FIrpic and FIracac.

interligand charge transfer, thus leading relatively low quantum efficiency. While for FIrpic, there is not ILCT involved in the process. To summarize above two likely reasons, FIrpic might exhibit higher efficiency than FIracac. The more detailed interpretation on efficiency will await rate constant calculations with inclusion of spin−orbit coupling effects.

Molecular Design. To achieve high phosphorescence efficiency materials, what we can do is to alter the metal complex structure based on the hints from our calculated results. So far dfppy has been well accepted as a good chelated ligand in blue phosphorescence metal complexes. Efforts on choosing appropriate ancillary ligands will be a proper route to go. The ancillary ligands should be asymmetric structures with a larger HOMO−LUMO energy gap than dfppy. And also the interaction strength of the ligand and central metal should be strong enough to lower the HOMO and LUMO energy levels. An ancillary ligand with proper modification of pic or mimics of pic probably improves the blue phosphorescence efficiency greatly.

Conclusion

In summary, from our calculation results, we have characterized all of the low-lying electronic states as admixture of MLCT and ILCT in character. In these states, the common features are that the HOMOs of the metal complexes are Ir(5d) character (about 50% in composition) with a significant admixture of ligand π orbitals. The effect of ancillary ligands on tuning the color emission is interpreted in terms of the raising/lowering of HOMOs and LUMOs as well as the gaps between them.

Finally we should emphasize two points regarding the present calculations. First, our calculation results pertain both to the ground and excited states geometries. The luminescence properties reflect the significant geometry changes in the excited state. It is different from previous study on $Ir(ppy)_3$ in which only the ground state is considered by ignoring the geometry change between the ground and excited states.[15a] Second, the more detailed interpretation of effects such as phosphorescence properties will await the inclusion of spin−orbit coupling effects, which are not included in present results.

Acknowledgment. We thank the financial support from the National Nature Science Foundation of China. (Grant Nos. 20573040, 20474024, 20603013, 20704015, 90501001, and 50303007), Ministry of Science and Technology of China (Grant No. 2002CB6134003), and PCSIRT. Computational resources from the Institute of Theoretical Chemistry of Jilin University are highly appreciated.

References and Notes

(1) (a) Stufkens, D. J.; Aarnts, M. P.; Rossenaar, B. D.; Vlcek, A. *Coord. Chem. Rev.* **1998**, *177*, 127. (b) Ranjan, S.; Lin, S.-Y.; Hwang, K.-C.; Chi, Y.; Ching, W.-L.; Liu, C.-S.; Tao, Y.-T.; Chien, C.-H.; Peng, S.-M.; Lee, G.-H. *Inorg. Chem.* **2003**, *42*, 1248.

(2) (a) Balzani, B.; Juris, A. *Coord. Chem. Rev.* **2001**, *211*, 97. (b) Welter, S.; Brunner, K.; Hofstraat, J. W.; De Cola, L. *Nature* **2003**, *421*, 54.

(3) Chou, P.-T.; Chi, Y. *Chem. Eur. J.* **2007**, *13*, 380.

(4) (a) Baldo, M. A.; Thompson, M. E.; Forrest, S. R. *Nature* **2000**, *403*, 750. (b) Lo, S. C.; Male, N. A. H.; Markham, J. P. J.; Magennis, S. W.; Burn, P. L.; Salata, O. V.; Samuel, I. D. W. *Adv. Mater.* **2002**, *14*, 975. (c) Tamayo, A. B.; Alleyne, B. D.; Djurovich, P. I.; Lamansky, S.; Tsyba, I.; Ho, N. N.; Bau, R.; Thompson, M. E. *J. Am. Chem. Soc.* **2003**, *125*, 7377. (d) Yeh, S.-J.; Wu, M.-F.; Chen, C.-T.; Song, Y.-H.; Chi, Y.; Ho, M. -H.; Hsu, S. -F.; Chen, C. H. *Adv. Mater.* **2005**, *17*, 285. (e) Yang, C.-H.; Cheng, Y. M.; Chi, Y.; Hsu, C.-J.; Fang, F.-C.; Wong, K.-T.; Chou, P.-T.; Chang, C.-H.; Tsai, M.-H.; Wu, C.-C. *Angew. Chem., Int. Ed.* **2007**, *46*, 2418.

(5) Nazeeruddin, M. K.; Angelis, F. D.; Fantacci, S.; Selloni, A.; Viscardi, G.; Liska, P.; Ito, S.; Takeru, B.; Gratzel, M. *J. Am. Chem. Soc.* **2005**, *127*, 16835.

(6) (a) Adachi, C.; Baldo, M. A.; Forrest, S. R.; Lamansky, S.; Thompson, M. E.; Kwong, R. C. *Appl. Phys. Lett.* **2001**, *78*, 1622. (b) Lamansky, S.; Djurovich, P.; Murphy, D.; Abdel-Razzaq, F.; Lee, H.-E.; Adachi, C.; Burrows, P. E.; Forrest, S. R.; Thompson, M. E. *J. Am. Chem. Soc.* **2001**, *123*, 4304.

(7) (a) Tang, Y.; Tehan, E. C.; Tao, Z.; Bright, F. V. *Anal. Chem.* **2003**, *75*, 2407. (b) DeRosa, M. C.; Mosher, P. J.; Yap, G. P. A.; Focsaeanu, K.-S.; Crutchley, R. J.; Evans, C. E. B. *Inorg. Chem.* **2003**, *42*, 4864.

(8) (a) Nazeeruddin, M. K.; Humphry-Baker, R.; Berner, D.; Rivier, S.; Zuppiroli, L.; Graetzel, M. *J. Am. Chem. Soc.* **2003**, *125*, 8790. (b) Li, C.-L.; Su, Y.-J.; Tao, Y.-T.; Chou, P.-T.; Chien, C.-H.; Cheng, C.-C.; Liu, R.-S. *Adv. Funct. Mater.* **2005**, *15*, 387. (c) Rayabarapu, D. K.; Paulose, B. M. J. S.; Duan, J.-P.; Cheng, C.-H. *Adv. Mater.* **2005**, *17*, 349. (d) Li, H.-C.; Chou, P.-T.; Hu, Y.-H.; Cheng, Y.-M.; Liu, R.-S. *Organometallics* **2005**, *24*, 1329. (e) Okada, S.; Okinaka, K.; Iwawaki, H.; Furugori, M.; Hashimoto, M.; Mukaide, T.; Kamatani, J.; Igawa, S.; Tsuboyama, A.; Takiguchi, T.; Ueno, K. *Dalton Trans.* **2005**, *9*, 1583. (f) Wong, W.-Y.; Zhou, G.-J.; Yu, X.-M.; Kwok, H.-S.; Tang, B.-Z. *Adv. Funct. Mater.* **2006**, *16*, 838.

(9) (a) Beeby, A.; Bettington, S.; Samuel, I. D. W.; Wang, Z. J. *J. Mater. Chem.* **2003**, *13*, 80. (b) Jung, S.; Kang, Y.; Kim, H.-S.; Kim, Y.-H.; Lee, C.-L.; Kim, J.-J.; Lee, S.-K.; Kwon, S.-K. *Eur. J. Inorg. Chem.* **2004**, *43*, 3415. (c) You, Y.; Park, S. Y. *J. Am. Chem. Soc.* **2005**, *127*, 12438. (d) Liang, B.; Jiang, C.; Chen, Z.; Zhang, X.; Shi, H.; Cao, Y. *J. Mater. Chem.* **2006**, *16*, 1281.

(10) (a) Lee, C.; Das, R. R.; Kim, J. *Chem. Mater.* **2004**, *16*, 4642. (b) Li, J.; Djurovich, P. I.; Alleyne, B. D.; Yousufuddin, M.; Ho, N. N.; Thomas, J. C.; Peters, J.; Bau, R.; Thompson, M. E. *Inorg. Chem.* **2005**, *44*, 1713. (c) Takizawa, S.-Y.; Nishida, J.-I.; Tsuzuki, T.; Tokito, S.; Yamashita, Y. *Inorg. Chem.* **2007**, *46*, 4308.

(11) (a) Tokito, S.; Iijima, T.; Suzuri, Y.; Kita, H.; Tsuzuki, T.; Sato, F. *Appl. Phys. Lett.* **2003**, *83*, 569. (b) Holmes, R. J.; DOAndrade, B. W.; Forrest, S. R.; Ren, X.; Li, J.; Thompson, M. E. *Appl. Phys. Lett.* **2003**, *83*, 3818. (c) Ren, X.; Li, J.; Holmes, R. J.; Djurovich, P. I.; Forrest, S. R.; Thompson, M. E. *Chem. Mater.* **2004**, *16*, 4743.

(12) Lyu, Y.-Y.; Byun, Y.; Kwon, O.; Han, E.; Jeon, W. S.; Das, R. R.; Char, K. *J. Phys. Chem. B* **2006**, *110*, 10303.

(13) (a) Koike, K.; Okoshi, N.; Hori, H.; Takeuchi, K.; Ishitani, O.; Tsubaki, H.; Clark, I. P.; George, M. W.; Johnson, F. P. A.; Turner, J. J. *J. Am. Chem. Soc.* **2002**, *124*, 11448. (b) Zalis, S.; Farrell, I. R.; Vlcek, A. *J. Am. Chem. Soc.* **2003**, *125*, 4580.

(14) (a) Polson, M.; Ravaglia, M.; Fracasso, S.; Garavelli, M.; Scandola, F. *Inorg. Chem.* **2005**, *44*, 1282. (b) Tamayo, A. B.; Garon, S.; Sajoto, T.; Djurovich, P. I.; Tsyba, I. M.; Bau, R.; Thompson, M. E. *Inorg. Chem.* **2005**, *44*, 8723. (c) You, Y.; Park, S. Y. *J. Am. Chem. Soc.* **2005**, *127*, 12438. (d) Lo, S. C.; Shipley, C. P.; Bera, R. N.; Harding, R. E.; Cowley, A. R.; Burn, P. L.; Samuel, I. D. W. *Chem. Mater.* **2006**, *18*, 5119. (e) Zhao, Q.; Liu, S.; Shi, M.; Wang, C.; Yu, M.; Li, L.; Li, F.; Yi, T.; Huang, C. *Inorg. Chem.* **2006**, *45*, 6152.

(15) (a) Hay, P. J. *J. Phys. Chem. A* **2002**, *106*, 1634. (b) Yang, C.-H.; Li, S.-W.; Chi, Y.; Cheng, Y.-M.; Yeh, Y.-S.; Chou, P.-T.; Lee, G.-H.; Wang, C. H.; Shu, C. F. *Inorg. Chem.* **2005**, *44*, 7770. (c) Yang, C. H.; Su, W. L.; Fang, K. H.; Wang, S. P.; Sun, I. W. *Organometallics* **2006**, *25*, 4514. (d) Obara, S.; Itabashi, M.; Okuda, F.; Tamaki, S.; Tanabe, Y.; Ishii, Y.; Nozaki, K.; Haga, M.-A. *Inorg. Chem.* **2006**, *45*, 8907. (e) Liu, T.; Zhang, H.-X.; Xia, B.-H. *J. Phys. Chem. A.* **2007**, *111*, 8724.

(16) (a) Lee, C.; Yang, W.; Parr, R. G. *Phys. Rev. B* **1998**, *37*, 785. (b) Becke, A. D. *J. Chem. Phys.* **1993**, *98*, 5648.

(17) Adamo, C.; Barone, V. *J. Chem. Phys.* **1999**, *110*, 6158.

(18) Perdew, J. P.; Burke, K.; Ernzerhof, M. *Phys. Rev. Lett.* **1996**, *77*, 3865.

(19) (a) Adamo, C.; Scuseria, G. E.; Barone, V. *J. Chem. Phys.* **1999**, *110*, 2889. (b) Wathelet, V.; Preat, J.; Bouhy, M.; Fontaine, M.; Perpète, E. A.; André, J. M.; Jacquemin, D. *Int. J. Quantum Chem.* **2006**, *106*, 1853.

(20) (a) Yang, L.; Ren, A.-M.; Feng, J.-K.; Liu, X.-D.; Ma, Y.-G.; Zhang, H.-X. *Inorg. Chem.* **2004**, *43*, 5961.

(21) (a) Yang, C.-H.; Li, S.-W.; Chi, Y.; Cheng, Y.-M.; Yeh, Y.-S.; Chou, P.-T.; Lee, G.-H.; Wang, C.-H.; Shu, C.-F. *Inorg. Chem.* **2005**, *44*, 7770. (b) Angelis, F. D.; Fantacci, S.; Evans, N.; Klein, C.; Zakeeruddin, S. M.; Moser, J.-E.; Kalyanasundaram, K.; Bolink, H. J.; Grätzel, M.; Nazeeruddin, M. K. *Inorg. Chem.* **2007**, *46*, 5989. (c) Dragonetti, C.; Falciola, L.; Mussini, P.; Righetto, S.; Roberto, D.; Ugo, R.; Valore, A.; Angelis, F. D.; Fantacci, S.; Sgamellotti, A.; Ramon, M.; Muccini, M. *Inorg. Chem.* **2007**, *46*, 8533.

(22) Frisch, A. E.;. Frisch, M. J. *Gaussian 98 User's Reference*; Gaussian Inc.: Pittsburgh, PA, 1998. see also references therein.

(23) (a) Koch, W.; Holthausen, M. C. *A Chemist's Guide to Density Functional Theory*; Wiley-VCH: Weinheim, Germany, 2000. (b) Hay, P. J.; Walt, W. R. *J. Chem. Phys.* **1985**, *82*, 299.

(24) (a) Nam, E. J.; Kim, J. H.; Kim, B.; Kim, S. M.; Park, N. G.; Kim, Y. S.; Kim, Y. K.; Ha, Y. *Bull. Chem. Soc. Jpn.* **2004**, *77*, 751. (b) Park, N. G.; Choi, G. C.; Lee, J. E.; Kim, Y. S. *Curr. Appl. Phys.* **2005**, *5*, 79. (c) Lee, Y. H.; Kim, Y. S. *Curr. Appl. Phys.* **2007**, *7*, 504.

(25) Frisch, M. J.; Trucks, G. W.; Schlegel, H. B.; Scuseria, G. E.; Robb, M. A.; Cheeseman, J. R.; Montgomery, J. A., Jr.; Vreven, T.; Kudin, K. N.; Burant, J. C.; Millam, J. M.; Lyengar, S. S.; Tomasi, J.; Barone, V.; Mennucci, B.; Cossi, M.; Scalmani, G.; Rega, N.; Petersson, G. A.; Nakatsuji, H.; Hada, M.; Ehara, M.; Toyota, K.; Fukuda, R.; Hasegawa, J.; Ishida, M.; Nakajima, T.; Honda, Y.; Kitao, O.; Nakai, H.; Klene, M.; Li, X.; Knox, J. E.; Hratchian, H. P.; Cross, J. B.; Bakken, V.; Adamo, C.; Jaramillo, J.; Gomperts, R.; Stratmann, R. E.; Yazyev, O. ; Austin, A. J. ; Cammi, R. ; Pomelli, C. ; Ochterski, J. W. ; Ayala, P. Y. ; Morokuma, K. ; Voth, G. A. ; Salvador, P. ; Dannenberg, J. J. ; Zakrzewski, V. G. ; Dapprich, S. ; Daniels, A. D. ; Strain, M. C. ; Farkas, O. ; Malick, D. K. ; Rabuck, A. D. ; Raghavachari, K. ; Foresman, J. B. ; Ortiz, J. V. ; Cui, Q. ; Baboul, A. G. ; Clifford, S. ; Cioslowski, J. ; Stefanov, B. B. ; Liu, G. ; Liashenko, A. ; Piskorz, P. ; Komaromi, I. ; Martin, R. L. ; Fox, D. J. ; Keith, T. ; Al-Laham, M. A. ; Peng, C. Y. ; Nanayakkara, A. ; Challacombe, M. ; Gill, P. M. W. ; Johnson, B. ; Chen, W. ; Wong, M. W. ; Gonzalez, C. ; Pople, J. A. *Gaussian 03, revision B.05*; Gaussian, Inc.: Wallingford, CT, 2004.

(26) The standard deviations are calculated though the formula $\sigma = ((1/N)\sum_{i=1}^{N}(x_i - x_{exp}))^{1/2}$, where x_i is calculated result for each parameter, x_{exp} is the experimental value for the same parameter as x_i, and N is total number of the selected parameters for calculations.

(27) Park, N. G.; Choi, G. C.; Lee, Y. H.; Kim, Y. S. *Curr. Appl. Phys.* **2006**, *6*, 620.

(28) Gu, X.; Fei, T.; Zhang, H. Y. Ma, Y. G. Unpublished.

(29) Adachi, C.; Kwong, R. C.; Djurovich, P.; Adamovich, V.; Baldo, M. A.; Thompson, M. E.; Forrest, S. T. *Appl. Phys. Lett.* **2001**, *79*, 2082.

(30) Dedeian, K.; Shi, J.; Shepherd, N.; Forsythe, E.; Morton, D. C. *Inorg. Chem.* **2005**, *44*, 4445.

JP8026429